Advanced Powder Technology 28 (2017) 131–138

Contents lists available at ScienceDirect

Advanced Powder Technology

journal homepage: www.elsevier.com/locate/apt

Original Research Paper

Characterizations of nanostructured nickel aluminates as catalysts for conversion of glycerol: Influence of the preparation methods

Antonio S.B. Neto [a], Alcemira C. Oliveira [b,1], Josué M. Filho [b,1], Norma Amadeo [c], Maria L. Dieuzeide [c], Francisco F. de Sousa [d], Alcineia C. Oliveira [a,*]

[a] Universidade Federal do Ceará, Campus do Pici-Bloco 940, Departamento de Química Analítica e Fisioquímica, 60.000.000 Fortaleza, Ceará, Brazil
[b] Universidade Federal do Ceará, Campus do Pici-Bloco 922, Departamento de Física, Fortaleza, Ceará, Brazil
[c] ITHES CONICET-UBA, Buenos Aires, Argentina
[d] Universidade Federal do Pará, Campus Universitário de Marabá, Cep: 68505-080 Marabá, Pará, Brazil

ARTICLE INFO

Article history:
Received 14 August 2016
Received in revised form 18 September 2016
Accepted 21 September 2016
Available online 18 October 2016

Keywords:
Nickel aluminates
Nanostructures
Characterizations
Preparation method
Glycerol

ABSTRACT

Three different preparation methods were applied to prepare nickel aluminates (i.e. nanocasting (NiAlN), coprecipitation (NiAlC) and wet impregnation (NiAlW) methods). All catalysts exhibited the $NiAl_2O_4$ phase besides that of NiO and γ-Al_2O_3. The NiAlN catalyst showed nanoparticles of the aforesaid oxides whereas $NiAl_xO_y$ was the predominant phase found over NiAlW catalyst. The performances of the nickel aluminate-based catalysts were evaluated in glycerol dehydration to produce valuable chemical compounds through the dehydration of glycerol. The sintering effects were responsible for the decreased performance of NiAlC in glycerol dehydration. On the contrary, NiAlN is found to be deactivated due to the lesser stability of its supported nanoparticles, being the glycerol conversion of ca. 3.3% at the end of the reaction. Besides, the reaction efficiently proceeded on NiAlW, which had a high catalytic performance with 19.7% glycerol conversion to acetol and others products and no deactivation along of the time for 25 h of time on stream was observed. This was due to the stability of the $NiAl_xO_y$ phase, which impeded phase transformation and was resistant to heavy coking.

1. Introduction

Nickel aluminates can be synthesized by various preparation methods and they are very efficient catalysts or carries for the dehydration of a variety of alcohols: ethanol, glycerol, octanol, propanol, 4-hydroxy valeric, among other hydrocarbons [1–3]. It is a partially inverse spinel oxide structure with an ideal unit cell of a cubic system of $NiAl_2O_4$, being a class of chemically and thermally stable materials [2,3].

The role played by the structure of nickel aluminates for alcohol transformation reactions is not clear in the open literature, although several papers showed the Ni^{2+} centers are very efficient to convert the alcohols through the cleavage of the C—C, O—H and C—H bonds [4–6].

Moreover, the catalytic properties of the nickel aluminates depend on the preparation method, calcination temperature, among other aspects [5–7]. Therefore, the design of active, selective and recyclable nickel aluminate catalyst for glycerol dehydration is a challenging goal in the field of dehydration catalysis.

In this context, several attempts have been made by researchers for exploitation of uses for glycerol [8–11]. The dehydration of the tri-alcohol reaction constitutes an important research area because it represents the core of a variety of chemical processes to convert the trialcohol into valuable products such acrolein or acetol [12,13]. Acrolein (2-propenal) is a very useful chemical intermediate with widespread applications in antifreeze, polyester fibers, resins, pharmaceuticals, cosmetics, flavors and fragrances, among others whereas acetol (1-hydroxyacetone) is widely used as organic synthesis intermediate for polyols and used in food and cosmetic industry products [10].

The acetol formation through dehydration of glycerol is observed, when catalysis possessing Lewis acidity, or strong basic sites on their surface are used and this reaction occurs via protonation of the terminal hydroxyl group of glycerol with consecutive elimination of water molecule and formation of an enol intermediate [11,13]. Considering the acrolein production by dehydration of glycerol, catalysts having Brønsted acid sites give high acrolein selectivity [12]. In this direction, a variety of catalysts such as oxi-

* Corresponding author. Fax: +55 85 33 66 90 51/9982.
E-mail address: alcineia@ufc.br (A.C. Oliveira).
[1] Fax: +55 85 33 66 94 83.

http://dx.doi.org/10.1016/j.apt.2016.09.013
0921-8831/

des, sulfates, metal-based catalysts, phosphates, niobic acid, heteropolyacids, hydrotalcite-type compounds and silica and alumina supported solids, zeolites have been investigated [11,14–16]. Since these catalysts suffer from particle sintering, leaching of the active sites or even carbon deposition, there is a great interest for the development of alternative catalysts. This is a very important factor regarding a possible catalysts' commercial application.

In contrast with the huge research effort focused in the recent years to find out new catalytic applications of nickel aluminates material, almost no papers can be found in the open literature dealing with the nickel aluminate deactivation in dehydration of glycerol. As observed in steam reforming process and glycerol hydrogenolysis, the significant features of $NiAl_2O_4$ oxide catalysts includes elevated textural properties, profound redox and acid–base properties, high thermal stability and strong mechanical strength [2,3]. In addition, Ni/Al_2O_3 based catalysts have been used widely in glycerol steam reforming and *in situ* transformations lead to active $Ni^o/NiAl_2O_4$ phase [1,5]. However, the changes in Ni particle sizes and morphologies during the reaction and the interactions between the alumina carrier and the supported metal may result in detrimental effects such as coking and sintering for the catalyst.

Thus, in this paper, nanostructured nickel aluminates obtained by three preparation methods are evaluated in gas phase dehydration of glycerol. Many different synthetic procedures have been developed to obtain nickel aluminates. Among them, solid-state reaction (ceramic method) and aqueous solution (wet chemical method) such as coprecipitation and sol-gel methods are extensively studied [5,17,18]. The main advantages of wet chemical methods are increased homogeneity and high surface area of the resulting precipitate or gel, which lead to smaller particle size. Emphasis was given in the correlation between the structural properties of the solids after the reaction and their catalytic performance.

2. Experimental

2.1. Preparation of the catalysts

Three wet methods were used for the preparation of the catalysts containing about 10–12 wt% of Ni: coprecipitation, nanocasting and wet impregnation .

The NiAlC catalyst was prepared by the coprecipitation of metal nitrates method. Under stirring, a 10% aqueous solution of aluminum nitrate ($Al(NO_3)_3{\cdot}9H_2O$ Reagen, 99 wt%) and nickel nitrate ($Ni(NO_3)_2{\cdot}6H_2O$, Vetec, 99 wt%) were added slowly with vigorous stirring into a sodium carbonate and sodium hydroxide solutions at room temperature. Then, the pH of the final mixture was adjusted to 11 by dropping a 1 $mol{\cdot}L^{-1}$ aqueous solution of sodium hydroxide. After stirring and standing the colloidal mixture for 1 h, the resulting precipitate was aged at 60 °C for additional 2 h and then was filtered, washed with deionized water several times until the pH reached 7, dried at 80 °C overnight and calcined in air flow at 700 °C using a heating rate of 1 °C min^{-1} for 6 h.

In case of NiAlW, the catalyst was prepared by the incipient wetness impregnation method studied [5]. For this purpose, aqueous solution of $Ni(NO_3)_2{\cdot}6H_2O$ (99% Merck) was prepared and γ-Al_2O_3 (Rhone Poulenc) was used. The γ-Al_2O_3 was impregnated with 10% of Ni and the subsequent drying of the samples was performed in a muffle at 120 °C for 6 h, followed by the calcination from room temperature to 700 °C using a heating rate of 1 °C min^{-1} and held at 700 °C for 6 h.

For nanocasted NiAlN, the preparation method was based on previous work [19]. The synthesis was performed at constant pH in the presence of 10 g of each metal source e.g., nickel acetate and tri-sec butoxide, which were dissolved in isopropanol, under vigorous stirring. After adding the solutions, about 1.0 g of silica template was dispersed in 40 mL of n-hexane with stirring for 3 h. Then, the obtained slurry was added dropwise to 1 mL of the metal precursor solutions with vigorous stirring for 24 h. The resulting mixture was then isolated by filtration and washed with water, being dried afterwards. The prepared solid was calcined at 700 °C with a heating rate of 1 °C min^{-1} and maintained at that temperature for 6 h, under nitrogen flow. The template was partially removed by stirring the composite in a 5% HF solution and further washed with ethanol, filtered and dried to obtain the resultant oxide sample.

2.2. Characterization of the catalysts

The NiAlC and NiAlN catalysts were characterized by chemical analysis (ICP-OES), X-ray diffraction (XRD), N_2 adsorption isotherms, Raman spectroscopy, and Transmission Electron Microscopy (TEM) techniques.

The chemical analyses of the solids were performed by inductively coupled plasma optical emission spectroscopy (ICP-OES). The analyses were carried out with a Shimadzu ICPS-7500 spectrometer. About 100 mg of the solid was prepared by dissolution in concentrated nitric acid. The precipitated formed was diluted again in a 1% nitric acid solution to perform the measurements.

XRD analyses of fresh solids were performed on a Rigaku (DMAXB model) diffractometer with Cu Kα radiation (40 kV and 30 mA). The diffractograms can be found in the papers published elsewhere [3,19,20]. The spent solids used in the reaction were also characterized by XRD and the diffraction pattern was identified through comparison with those included in the ICDD (International Center of Diffraction Data) database. Moreover, characterizations of fresh NiAlW catalyst (XRD and chemical analyses) are found in a previous paper [20].

The nitrogen adsorption isotherms at −196 °C were carried out using a Bel Japan, BELSORP Mini II. Before adsorption measurements, samples (ca. 0.05 g) were heated at 200 °C for 4 h under nitrogen flow. Surface areas of the fresh and spent solids were calculated by the Brunauer–Emmett–Teller (BET) method and pore diameters were obtained by BJH method. The surface areas of the microporous solids were measured by t-plot method.

Raman spectra of the fresh and spent catalysts were obtained using a T64000 Jobin Ivon spectrometer. Approximately, 10 mg of each sample was used with an argon laser at 514.5 nm and a power of 10 mW. Raman spectrum of NiAlC and NiAlW samples were obtained in a Horriba Jobin Yvon Labram1000 microscope with a 514.5 nm laser line. The power of 10 mW using a 100 times objective and a 600 mm^{-1} grating were applied.

The Transmission Electron Microscopy (TEM) images of the spent solids were obtained on a FEI Tecnai transmission electron microscope at 120 kV with a resolution of 0.17 nm. Previously, samples were dispersed in ethanol and placed in the grids to perform the analyses.

2.3. Activity testing

The gas-phase dehydration of glycerol was typically conducted at 250 °C, P = 1 atm, using 100 mg of catalyst. The reactant 20wt% of aqueous solution of glycerol was introduced in the in a fix bed reactor and the reaction was carried out at 250 °C. The products of the reaction were analyzed by a G-Crom chromatograph. The products were identified by gas chromatography coupled to mass spectrometry (GC–MS). According to the findings [21–23], conversion of glycerol and selectivities to the products can be obtained as follows:

$$\%\text{Glycerol conversion} = \frac{\text{moles of glycerol reacted}}{\text{moles of glycerol in the feed}} \times 100 \quad (1)$$

$$\%\text{Product selectivity} = \frac{\text{moles of carbon in specific product}}{\text{moles of carbon in glycerol reacted}} \times 100 \quad (2)$$

3. Results and discussion

3.1. Structural and textural features of fresh solids

Fig. 1 illustrates the Raman spectra of the fresh solids.

The spectrum of NiAlN exhibits an intense and broad line at around 520 cm^{-1}, accompanied by lower wavenumber modes at about 187, 254 and 342 cm^{-1}. The broad lines of the spectrum confirm the XRD results that showed the solid has low crystallinity. The vibration at around 187 cm^{-1} is attributed to the E_g while those at lower wavenumber are due to T_{2g} modes from NiO [21,23]. The modes representing a large structured band extending from 372 to 650 cm^{-1} may be assigned to the normal cubic spinel with *Fd3m* space group of $NiAl_2O_4$ [21]. When assessing the long-range correlation for the arrangements of atoms, it can be inferred that NiAlN has only symmetric respiration modes of $NiAl_2O_4$ besides those of NiO.

The NiAlW has almost the same features of NiAlN in terms of the presence of the aforesaid vibrations, although the modes have major intensities in the former solid. The vibrations at around 264, 509, 564 and 658 cm^{-1} attributed to be from both $NiAl_xO_y$ and $NiAl_2O_4$ [23,24] are mostly missing in the spectrum. The features of the spectrum are nearly of NiO, mainly for the modes at about 77, 188 and 436 cm^{-1}. This is probably due to the impregnation process of the solids that promotes the dispersion of fine NiO, $NiAl_xO_y$ and $NiAl_2O_4$ particles on the γ-Al_2O_3 support surface. As consequence, the modes of the nickel aluminates experience a hardening in reason of the interaction with the support. Nevertheless, the NiAlC spectrum reveals clear differences comparing with the NiAlW and NiAlN. Raman measurements of NiAlC reveal a spectral feature with low intensity modes that can be attributed to NiO and $NiAl_2O_4$. However, the positions of NiO and $NiAl_2O_4$ modes are maintained and they are narrower suggesting that the sites are well defined due to the high crystallinity of the bulk.

The textural properties of the fresh solids are illustrated in Fig. 2.

The NiAlN displays a mesoporous character with relatively large pore sizes e.g., 2.4 nm. Assuming that the nanocasting method afford to high textural properties, the surface area of ca.400 $m^2\ g^{-1}$. Such features was used earlier for describing a type IV isotherm [20]. The pore volume of 1.2 $cm^3\ g^{-1}$ is expected due to the nano-sized character of the solid provided by the preparation method. There is no significant evidence of the amorphous silica remaining in the solid (neither observed by Raman nor XRD) could block the pores and prevent the final formation of an ordered nickel aluminate structure. The textural properties of NiAlW indicate the formation of micropores in addition to the presence of mesopores [23].

Although the surface areas, pore volume and diameters of NiAlW are lesser than that of NiAlN, BET surface area and pore volume values correlated well with the nanosized feature of dispersed nanoparticles in alumina support, as suggested by Raman results. The lowest textural properties are shown by NiAlC, which can be most likely explained by the sizes of its crystallites of ca. 22 nm for $NiAl_2O_4$ and 32 nm attributed to be from NiO phase, as further shown by XRD. These values illustrates that large particles are formed, having the solid a bulk feature [21,23].

The summary of the physicochemical properties of the solids is displayed in Table 1.

The ICP-OES results (Table 1) shows that the Ni content is about 10 wt% for NiAlW and NiAlC while Ni composition of NiAlN is about 12 wt% .

XRD features of nanocasted NiAlN composite displays the high-angle reflection peaks, which are typical of NiO cubic structure (ICDD 4-0835) and γ-Al_2O_3 (ICDD 50-741), as previously published [3]. Reflections with low intensity of cubic $NiAl_2O_4$ phase are also detected, which points to very small or poorly crystalline particles [19]. In case of the solid obtained by wet impregnation namely, NiAlW, wide reflections of low intensity can be associated with non-stoichiometric $NiAl_xO_y$ spinel phase and there is also broad contribution from stoichiometric $NiAl_2O_4$ one in some regions of the diffractogram [20]. The XRD patterns of NiAlC obtained by coprecipitation most likely consists of very high intense peaks related to $NiAl_2O_4$ crystallites [12]. However, because of the overlap with the NiO and γ-Al_2O_3 peaks, a reliable estimation of the relative amount of $NiAl_2O_4$ cannot be made.

According to the TEM results of the fresh NiAlC and NiAlN [12,20,24], three sets of lattice stripes and planes of 0.21, 0.64 and 0.34 nm are found, which are attributed to be from NiO, $NiAl_2O_4$ and γ-Al_2O_3, respectively. The mean size of the spinel phases is about 29 and 13.6 nm, respectively for NiAlC and NiAlN. In case of NiAlW, the same phases observed by XRD are suggested by TEM with the spinel ones having sizes of 10- and 5 nm, respectively for $NiAl_2O_4$ and $NiAl_xO_y$.

In summary, the Raman, XRD and TEM data agreed that the contribution of $NiAl_2O_4$ appeared in the diffractogram of the wet impregnated nickel aluminates and nanocasted. In contrast, a very small contribution of aforesaid phase is observed for the solid obtained by co-precipitation, being the peaks more intense than the others samples and thus the solid has high crystallinity.

3.2. Catalytic results in glycerol dehydration

Fig. 3 depicts the glycerol conversion versus time on stream, when the nickel aluminates derived catalysts are tested in the process of dehydration of glycerol. After 1 h on stream, all catalysts are actives in the reaction. NiAlN catalyst shows a glycerol conversion of 10% and it gradually drops to 3.3% in 25 h of time on stream. XRD and Raman measurements of NiAlN suggest that the nanoparticles of spinel-type $NiAl_2O_4$ or $NiAl_xO_y$ phases are supported on the mesoporous silica matrix [19], and additional Ni^{2+} atoms may have migrated into the Al_2O_3 to form the nickel aluminates [25–28]. As found elsewhere [3], small and well dispersed Ni^o crystallites coming from Ni^{2+} reduction can be formed during glycerol transformation reactions and promotes a noticeable coke formation. Thereby, the coking effects might be responsible for the decreased performance of the solid (further shown by Raman spectroscopy of spent solid). It is worthy to say that the conversion of glycerol obtained over NiAlN is lower than that tested using a 10% aqueous solution of glycerol (e.g. 50% of glycerol conversion for 6 h of reaction) [19]. As the amount of glycerol is lesser than that of current work, this suggests that more active sites on surface are available and contributed to the overall glycerol conversion. Also, it evidences that the Ni^{2+} coming from NiO and $NiAl_2O_4$ active phases are required to fully convert the molecules of the trialcohol.

On the contrary, NiAlC is found to be little more active catalyst due to the higher stability of their large particles (latter shown by TEM of spent solids). However, NiAlC exhibits identical behavior of NiAlN in terms of deactivation, being the glycerol conversion is about 8.4% at the end of the reaction (Table 2). Even if the Ni^{2+} species in the form of large particles are neither highly dispersed nor interact strongly with the support, the structural features of NiAlC lead to a slight higher conversion than that of NiAlN because of the

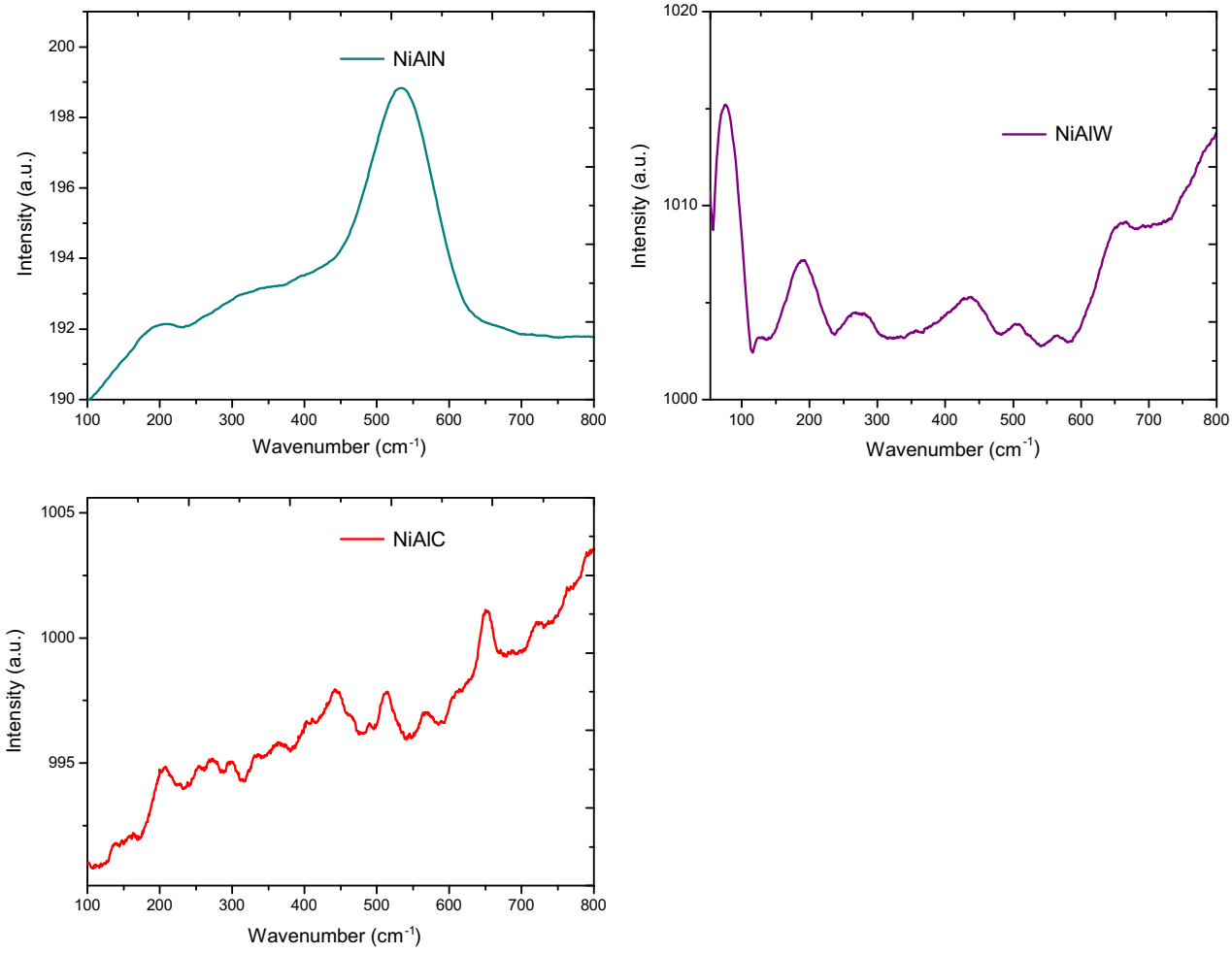

Fig. 1. Raman spectra of the fresh solids.

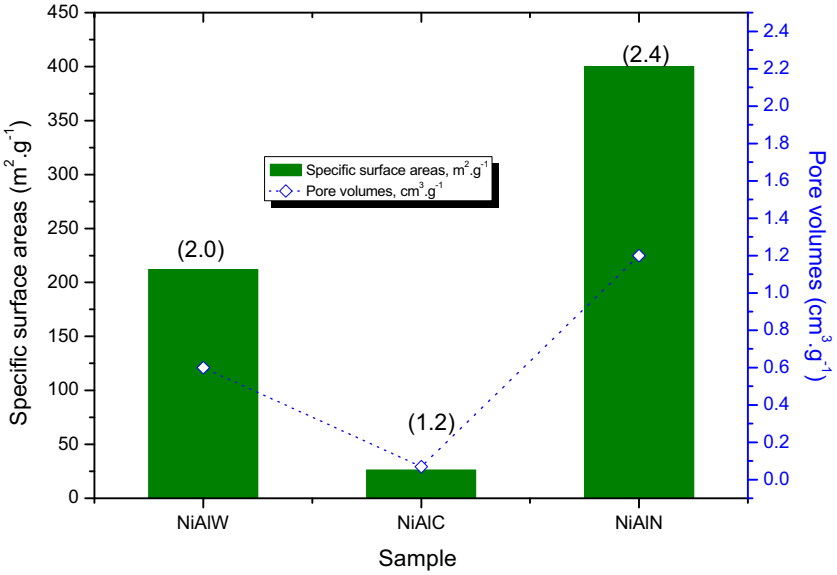

Fig. 2. Textural properties of fresh solids. The values in parenthesis are the pore sizes of the samples.

Table 1
Summary of the physicochemical characterizations of the fresh solids. The values in parenthesis are the sizes of the spinel phase particles obtained by TEM.

Sample	%Ni by ICP-OES	Phases found by XRD	TEM features
NAlW	10.1	NiO; $NiAl_xO_y$; $NiAl_2O_4$	NiO; $NiAl_xO_y$ (5); $NiAl_2O_4$ (10)
NiAlC	10.7	NiO; γ-Al_2O_3; $NiAl_2O_4$	NiO; γ-Al_2O_3; $NiAl_2O_4$ (29)
NiAlN	11.8	NiO; γ-Al_2O_3; $NiAl_2O_4$	NiO; γ-Al_2O_3; $NiAl_2O_4$ (13.6)

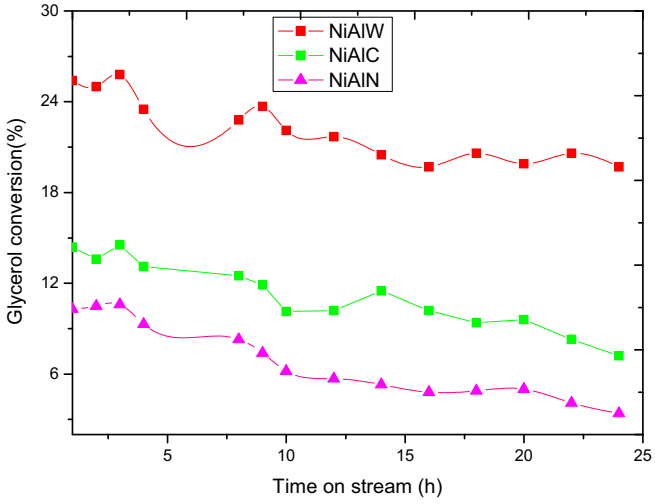

Fig. 3. Catalytic runs for the nickel aluminate based catalysts in the dehydration of glycerol. Reaction conditions: $T = 250$ °C, 20 wt% glycerol aqueous solution with 100 mg catalyst for 25 h reaction time.

Table 2
The textural properties of the solids, after the catalytic test.

Sample	Sg ($m^2 \cdot g^{-1}$)	Vp ($cm^3 \cdot g^{-1}$)
NAlW	198[a]	0.60
NiAlC	12[b]	0.03
NiAlN	107[a]	0.31

[a] BET method.
[b] t-plot.

catalyst ability to avoid coking on its surface, although sintering effects may be possible.

Furthermore, the reaction efficiently proceeds on NiAlW, which has a high catalytic performance with 24% glycerol conversion observed without catalyst deactivation along of the time on stream. The catalytic performance of NiAlW is due to the presence of $NiAl_xO_y$ prevailing over $NiAl_2O_4$ phase, even though the latter specie also promotes the reaction.

Studies on molecular sieves containing silica and alumina catalysts have shown that glycerol dehydration is favoured mainly by the alumina presence giving high acidity to solids [27,29]. As noticed elsewhere [26,27], although pure aluminas e.g., η-Al_2O_3, γ-Al_2O_3 are poorly actives in the reaction, the high selectivity to 1-hydroxyacetone over the aluminas is found be related to their largest amount of basic surface —OH groups and acid–base pair sites. Thus, even possessing γ-Al_2O_3 in their composition, the activity of the solids during the reaction could be not only due to alumina presence. Additionally, it can be suggested that the NiO phase is not sufficiently active in catalyzing glycerol dehydration, but apparently enhances glycerol hydrogenolysis, when partially reduced. This is consistent with previous reports where the volatile products by C—C hydrogenolysis of glycerol are formed [28–31]. The results obtained are therefore interpreted as $NiAl_xO_y$ can be explicitly the active phase for the reaction. Also, it is plausibly concluded that NiO and γ-Al_2O_3 species can promote the reaction, but either large particles or coke formation could lead to a decrease in the catalytic activity of NiAlC and NiAlN.

Table 2 also illustrates the products obtained in the condensable phase in the steady state condition. The major products detected in the liquid phase are 1-hydroxyacetone (acetol), acetone, ethanol and acetic acid. This demonstrates that glycerol can be dehydrated to acetol over the nickel aluminate catalysts, in spite of acrolein formation. On basic sites present in acidic catalysts, acetol is most likely formed with a decreased acrolein production, which occur with typical Brønsted acid catalysts [10,28,29]. There is no significant evidence of acrolein formation from GC analysis, since it could be involved in parallel reaction with glycerol or other products.

Moreover, oxidation products such as acetaldehyde, propanediols, aromatics and furane derivates are formed, namely others, mainly on NiAlC. In addition, the concentrations of gases such as methane, hydrogen, acrolein and CO_2 are very small over NiAlW and NiAlN and there may be attributed to the glycerol hydrogenolysis or aqueous reforming of glycerol reactions on Ni sites. This fact suggests that the free NiO coming from the catalysts is less active than that coming from the $NiAl_xO_y$ spinel oxide. Notably, the liquid production distribution is about 80% for NiAlW and NiAlN whereas the amount for NiAlC is around 55% with the concomitant decrease in the acetol production most likely due to the gas phase oxidation products or glycerol hydrogenolysis reactions.

It is also very important to highlight that the great quantities of 1-hydroxyacetone is formed in NiAlW, which undergoes a conversion of 19.7% at the end of reaction. Table 2 shows that the NiAlN gives similar product distributions with 3.4% of glycerol conversion in the steady state. As discussed before, this behavior is caused by the predominance of the presence of the $NiAl_xO_y$ spinel oxide phase in NiAlW. In contrast, NiAlC having a glycerol conversion of 8.4% displays a lesser acetol production than NiAlW and NiAlN. This implies that the NiO species of former catalyst i.e., the prevailing phase in the NiAlC, as seen by Raman and XRD results, require the hydrogen formed during the reaction to be reduced and form products from glycerol reforming or hydrogenolysis reactions. This hypothesis is confirmed further by the results obtained with the characterization of the spent catalysts.

3.3. Spent catalysts characterizations

XRD results of the spent solids are shown in Fig. 4.

After using the solids in the reaction, XRD pattern of NiAlN reveals an amorphous feature. This is a sound proof of the formation of heavy carbonaceous deposits during the reaction on solid surface, as further confirmed by Raman and TEM measurements. The XRD peaks of spent catalysts prepared by impregnation method are basically similar to that of $NiAl_2O_4$. For instance, the diffractogram displays two broad peaks at $2\theta = 37.2°$ (311), 44.9° (400) and 65.2° (440) from the spinel lattice possessing a cubic structure belonging to the Fd3 m space group. Even though XRD peaks do not exhibit clearly the presence of NiO, it cannot ensure its absence, since the peaks at around $2\theta = 36.3°$ (111), 43.1° (200) and 62.7° (440) assign the cubic NiO peaks, which could be overlapped with those of $NiAl_2O_4$. Furthermore, a board band about confirms the presence of carbonaceous species, most likely, the graphite at $2\theta = 25°$ (002) with the P63/mmc space group.

The XRD profile of spent NiAlC catalyst depicts a broad peak with no visible reflections and this can be associated with the

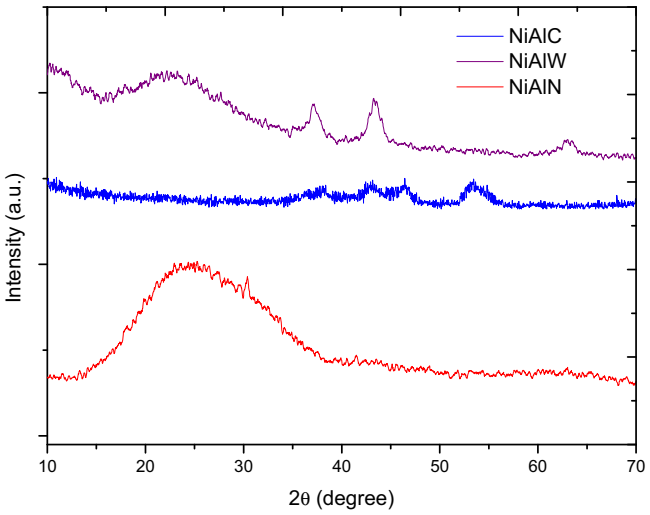

Fig. 4. XRD patterns of the spent solids used in the reaction for 25 h reaction time.

carbon deposition on solid surface, as latter shown by Raman analyses.

TEM micrographs of spent solids are performed to search for a deeper understanding of the particles' morphology (Fig. 5).

The micrograph of NiAlW (Fig. 5a) clearly exhibits very small particles (e.g., black dots in the image) with sizes ranging from 5 to 15 nm supported in a matrix e.g., gray plate. It may be assumed that these particles can be $NiAl_2O_4$ or $NiAl_xO_y$. Moreover, it can be rationalized that these particles do not suffered from sintering since their sizes do not change significantly compared to the fresh solid i.e. 3–10 nm. In addition, some crystallites that grow on top of the plate (supposed to be γ-Al_2O_3) are believed to be from Ni°. This confirms the assumptions taken in the catalytic results where free NiO is reduced to form light gases products.

TEM micrograph for NiAlN unveils an unlike dimensional structure for the particles, presenting continuous circular rings, which are assigned to carbon. The sequence of the images shows the appearance of large particles with loose agglomerated spherical shape. This consistent with the fact that the low activity of the sample is attributed to the presence of NiO and $NiAl_2O_4$ nanoparticles, which suffered from sintering and coking during the reaction.

TEM image of NiAlC displays large particles ranging from 12 to 50 nm and possessing with irregular spherical shape and loosely agglomerated. This is an evidence of sintering of NiO particles, which explain the decreased performance of the solid.

Textural properties after the catalytic test (Table 3) shows that NiAlC has a very low surface area of 12 $m^2 \cdot g^{-1}$ and pore volume of ca. 0.03 $cm^3 \cdot g^{-1}$ while NiAlN possesses BET surface area of ca. 107 $m^2 \cdot g^{-1}$ and pore volume of ca. 0.31 $cm^3 \cdot g^{-1}$, respectively.

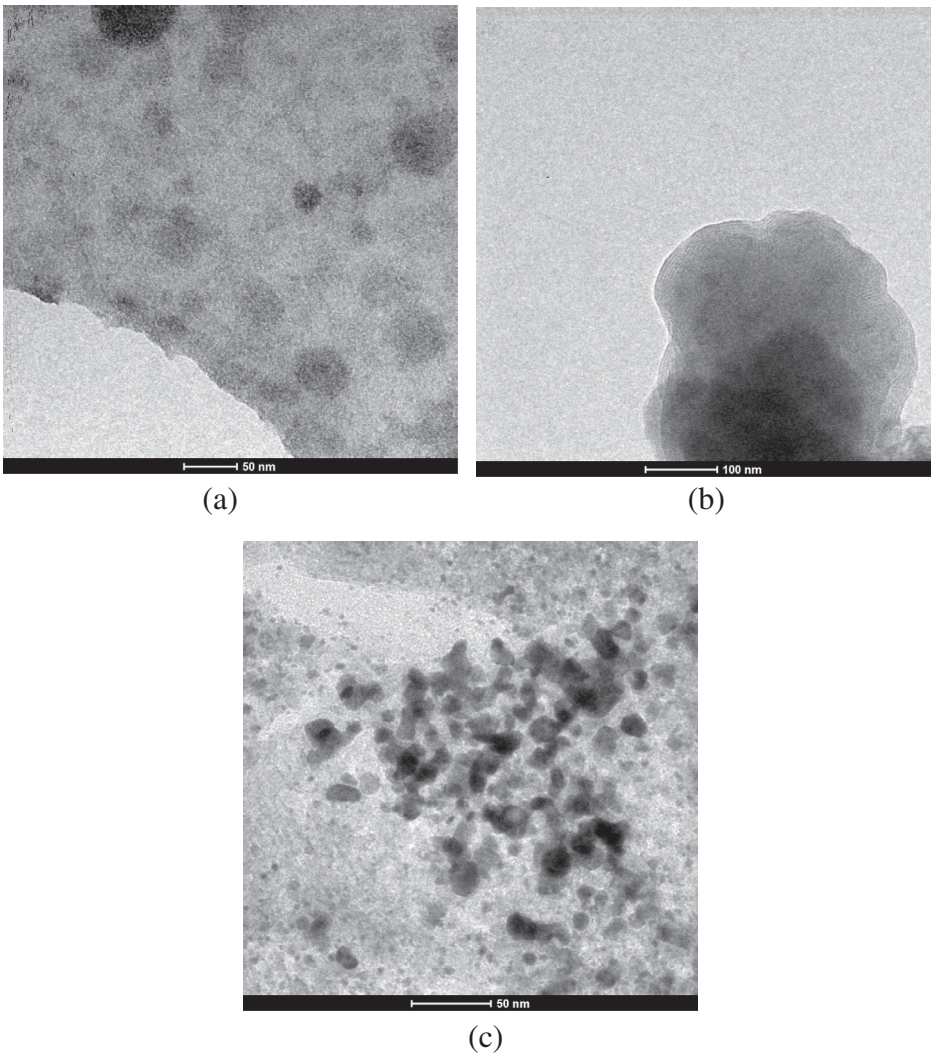

Fig. 5. TEM micrographs of the spent solids used in the dehydration of glycerol for 25 h reaction time: (a) NiAlW, (b) NiAlN and (c) NiAlC.

Table 3
Steady state conversion of glycerol in 25 h of reaction. Liquid products distribution in the dehydration of glycerol over NiAl-based catalysts. Operating conditions: 250 °C, 20 wt% glycerol aqueous solution with 100 mg catalyst for 25 h reaction time.

Catalyst	NiAlW	NiAlC	NiAlN
Conversion (%)	19.7	8.4	3.3
Products distribution (%)			
1-Hydroxyacetone	28.4	9.6	26.7
Acetic acid	20.0	5.3	22.6
Acetone	14.8	6.4	13.5
Ethanol	12.5	8.2	11.7
Others	7.1	25.3	6.2

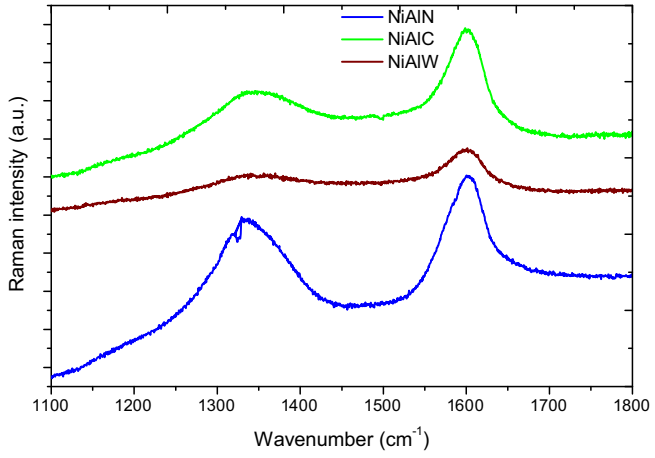

Fig. 6. Raman spectra of the spent catalysts for 25 h reaction time.

In contrast, NiAlW has the relatively large textural parameters after the catalytic test. Obviously, the values are lesser than that of fresh solids (Fig. 2). The decrease in the textural parameters of NiAlC and NiAlN can be attributed to the increase in particle sizes, as a consequence of the deactivation by sintering (or coking) during the glycerol transformation, as already predicted by TEM. It is clear that when the NiAlW is used in the reaction, glycerol conversion with time on stream is maintained. Thus, deactivation is less pronounced over this solid, which means that it is stable compared with NiAlN and NiAlC.

The vibrational properties of the spent solids are analyzed by Raman spectroscopy. Fig. 6 gives the Raman spectra of the solids, after being used in glycerol dehydration at 250 °C, 25 h of reaction with a 20 wt% aqueous solution of glycerol.

The Raman spectrum of spent NiAlN catalyst displays the disorder-induced planes of carbon and graphite bands at about 1330 cm^{-1} and 1590 cm^{-1}, respectively. They are attributed to be from the so called D and G bands. The distinctive border band at 1590 cm^{-1} appears in the spectrum, suggesting a very high amount of carbon species being richer in graphite carbon from glycerol decomposition [24]. Comparing with the spectrum of fresh catalyst (Fig. 1), it can be seen that the vibrational modes of $NiAl_2O_4$ and NiO at low wavenumbers are vanished due to carbon covering the solid surface. The spent NiAlC exhibits the same features as NiAlN, as observed by the Raman spectrum. However, a lesser amount of disordered carbon at around 1345 cm^{-1} is observed in the solid obtained by coprecipitation. The amount of the latter carbon species is higher than the graphite one, judging from the fact that the intensity of the D band is low. It can be either from heavy by-products glycerol dehydration formation or glycerol cracking reaction.

Carbon deposition seems inevitable on surface NiAlW, however, the catalyst is not severely damaged by coking, probably because its textural properties do not change drastically. Furthermore, the Raman spectrum shows that NiAlW maintain a structure (e.g., $NiAl_xO_y$), which does not suffer from phase transformation and is resistant to heavy coking.

The Ni^o specie can be formed by glycerol aqueous reforming parallel reaction [32] over NiAlW, according to the large amount of gaseous products formed only over this catalyst. The water vapor can act to reoxidize Ni^o to Ni^{2+} on the surface and thus, the good catalytic conversion and stability are observed in NiAlW. Contrary, the nanostructured NiAlN and bulk NiAlC are deactivated by carbonaceous deposits and phase transformation as shown by Raman, TEM and XRD measurements.

4. Conclusions

Among various nickel aluminate catalysts screened, the solid prepared by a wet impregnation method exhibited excellent catalytic performance for glycerol dehydration and also its hydrogenolysis. Acetol was largely produced over the solids while acrolein was produced in negligible level, which was possibly attributed to the parallel reaction involving glycerol and its derived compounds. The analogous coprecipitated and nanocasted catalysts had both NiO and $NiAl_2O_4$ phases, however sintering and coking effects caused the deactivation of the solids. Results suggested that $NiAl_2O_4$ phase improved dehydrogenation–hydrogenolysis reactions but nanosized $NiAl_xO_y$ active phase led to high glycerol conversions and catalytic stability.

Acknowledgments

The authors would like to acknowledge the CNPq (CNPq Grant no. 473568/2012-8), and the FUNCAP/CAPES Areas Estrategicas Program with Contract 23038.008860/2013-92.

References

[1] M.K. Nazemi, S. Sheibani, F. Rashchi, V.M. Gonzalez-DelaCruz, A. Caballero, Preparation of nanostructured nickel aluminate spinel powder from spent NiO/Al_2O_3 catalyst by mechano-chemical synthesis, Adv. Powder Technol. 23 (2012) 833–838.
[2] D. Visinescu, Papa, A.C. Ianculescu, I. Balint, O. Carp, Nickel-doped zinc aluminate oxides: starch-assisted synthesis, structural, optical properties, and their catalytic activity in oxidative coupling of methane, J. Nanopart. Res. 15 (2013) 1456.
[3] R.M. Freire, F.F. de Sousa, A.L. Pinheiro, E. Longhinotti, J.M. Filho, A.C. Oliveira, P.T.C. Freire, A.P. Ayala, A.C. Oliveira, Studies of catalytic activity and coke deactivation of spinel oxides during ethylbenzene dehydrogenation, Appl. Catal. A: Gen. 359 (2009) 165–179.
[4] L. Zhang, W. Li, J. Liu, C. Guo, Y. Wang, J. Zhang, Ethanol steam reforming reactions over Al_2O_3·SiO_2-supported Ni–La catalysts, Fuel 88 (2009) 511–518.
[5] M.L. Dieuzeide, M. Jobbagy, N. Amadeo, Glycerol steam reforming over Ni/Mg/γ-Al_2O_3 catalysts effect of Ni(II) content, Int. J. Hydrogen Energy 39 (2014) 16976–16982.
[6] S. Sepehri, M. Rezaei, Preparation of highly active nickel catalysts supported on mesoporous nanocrystalline γ-Al_2O_3 for methane autothermal reforming, Chem. Eng. Technol. 38 (2015) 1637–1645.
[7] A.H.M. Batista, F.S.O. Ramos, T.P. Braga, C.L. Lima, F.F. De Sousa, A.S. de Oliveira, E.B. Barros, J.R. de Souza, A. Valentini, J. Mendes Filho, A.C. Oliveira, Mesoporous MAl_2O_4 (M = Cu, Ni, Fe or Mg) spinels: characterisation and application in the catalytic dehydrogenation of ethylbenzene in the presence of CO_2, Appl. Catal. A:Gen. 382 (2010) 148–157.
[8] N.H. Tran, G.S. Kamali Kannangara, Conversion of glycerol to hydrogen rich gas, Chem. Soc. Rev. 42 (2013) 9454–9479.
[9] M. Kouzua, M. Tsunomori, S. Yamanaka, J. Hidaka, Solid base catalysis of calcium oxide for a reaction to convert vegetable oil into biodiesel, Adv. Powder Technol. 21 (2010) 488–494.
[10] C. Zhou–H, J.N. Beltramini, Y.-X. Fan, C.Q. Lu, Chemoselective catalytic conversion of glycerol as a biorenewable source to valuable commodity chemicals, Chem. Soc. Rev. 37 (2008) 527–549.
[11] D.C. Carvalho, L.G. Pinheiro, A. Campos, E.R.C. Millet, F.F. de Sousa, J.M. Filho, G. D. Saraiva, E.C. da Silva Filho, M.G. Fonseca, A.C. Oliveira, Characterization and catalytic performances of copper and cobalt-exchanged hydroxyapatite in

glycerol conversion for 1-hydroxyacetone production, Appl. Catal. A: Gen. 471 (2014) 39–49.
[12] C.-J. Yue, M.M. Gan, L.-P. Gu, Y-F. Zhuang, In situ synthesized nano-copper over ZSM-5 for the catalytic dehydration of glycerol under mild conditions, J. Taiwan Inst. Chem. Eng. 45 (2014) 1443–1448.
[13] A.S. de Oliveira, S.J.S. Vasconcelos, J.R. de Sousa, F.F. de Sousa, J.M. Filho, A.C. Oliveira, Catalytic conversion of glycerol to acrolein over modified molecular sieves: activity and deactivation studies, Chem. Eng. J. 168 (2011) 765–774.
[14] S. Chokkaram, R. Srinivasan, D.R. Milburn, B.H. Davis, Conversion of 2-octanol over nickel-alumina, cobalt-alumina, and alumina catalysts, J. Mol. Catal. A: Chem. 121 (1997) 157–169.
[15] I. Gandarias, P.L. Arias, J. Requies, M. El Doukkali, M.B. Güemez, Liquid-phase glycerol hydrogenolysis to 1,2-propanediol under nitrogen pressure using 2-propanol as hydrogen source, J. Catal. 282 (2011) 237–247.
[16] B. Dou, C. Wang, Y. Song, H. Chen, Y. Xu, Activity of Ni–Cu–Al based catalyst for renewable hydrogen production from steam reforming of glycerol, Energy Convers. Manage. 78 (2014) 253–259.
[17] A.A. Lemonidou, M.A. Goula, I.A. Vasalos, Carbon dioxide reforming of methane over 5 wt% nickel calcium aluminate catalysts – effect of preparation method, Catal. Today 46 (1998) 175–183.
[18] A. Tirsoaga, D. Visinescu, B. Jurca, A. Ianculescu, O. Carp, Eco-friendly combustion based synthesis of metal aluminates MAl_2O_4 (M = Ni, Co), J. Nanopart. Res. 13 (2011) 6397–6408.
[19] F.A.A. Barros, H.S.A. de Sousa, A.C. Oliveira, M.C. Junior, J.M. Filho, B.C. Viana, A. C. Oliveira, Characterisation of high surface area nanocomposites for glycerol transformation: effect of the presence of silica on the structure and catalytic activity, Catal. Today 212 (2013) 127–136.
[20] A. Romero, M. Jobbágy, M. Laborde, G. Baronetti, N. Amadeo, Ni(II)–Mg (II)–Al(III) catalysts for hydrogen production from ethanol steam reforming: influence of the Mg content, Appl. Catal. A:Gen. 470 (2014) 398–404.
[21] F.A.A. Barros, A.J.R. Castro, J.M. Filho, B.C. Viana, A. Campos, A.C. Oliveira, Characterisation and catalytic properties of Ni Co, Ce and Ru nanoparticles in mesoporous carbon spheres, J. Nanop. Res. 14 (2012) 1096.
[22] L.-Z. Tao, S.-H. Chai, Y. Zuo, W.-T. Zheng, Y. Liang, B.-Q. Xu, Sustainable production of acrolein: acidic binary metal oxide catalysts for gas-phase dehydration of glycerol, Catal. Today 158 (2010) 310–316.
[23] M.A. Laguna-Bercero, M.L. Sanjuna, R.I. Merino, Raman spectroscopic study of cation disorder in poly- and single crystals of the nickel aluminate spinel, J. Phys.: Condens. Matter 19 (2007) 186217.
[24] A.L. Pinheiro, A.N. Pinheiro, A. Valentini, J.M. Filho, F.F. de Sousa, J.R. de Sousa, M.G.C. Rocha, P. Bargiela, A.C. Oliveira, Analysis of coke deposition and study of the structural features of MAl_2O_4 catalysts for the dry reforming of methane, Catal. Commun. 11 (2009) 11–14.
[25] B. Valle, B. Aramburu, A. Remiro, J. Bilbao, A.G. Gayubo, Effect of calcination/reduction conditions of Ni/La_2O_3–α-Al_2O_3 catalyst on its activity and stability for hydrogen production by steam reforming of raw bio-oil/ethanol, Appl. Catal. B: Environ. 147 (2014) 402–410.
[26] Y.T. Kim, K.-D. Jung, E.D. Park, Gas-phase dehydration of glycerol over silica–alumina catalysts, Appl. Catal. B: Environ. 107 (2011) 177–187.
[27] J.P. Lourenço, A. Fernandes, R.A. Bértolo, M.F. Ribeiro, Gas-phase dehydration of glycerol over thermally-stable SAPO-40 catalyst, RSC Adv. 5 (2015) 10667–10674.
[28] W. Suprun, M. Lutecki, R. Gläser, H. Papp, Catalytic activity of bifunctional transition metal oxide containing phosphated alumina catalysts in the dehydration of glycerol, J. Mol. Catal. A: Chem. 342–343 (2011) 91–100.
[29] C.L. Lima, H.S.A. Sousa, S.J.S. Vasconcelos, J.M. Filho, A.C. Oliveira, F.F. Sousa, A. C. Oliveira, Effect of sulfatation on the physicochemical and catalytic properties of molecular sieves, React. Kinet. Mechan. Catal. 102 (2011) 102487–102500.
[30] B.C. Miranda, R.J. Chimentão, J.B.O. Santos, F. Gispert-Guirado, J. Llorca, F. Medina, F. López Bonillo, J.E. Sueiras, Conversion of glycerol over 10%Ni/γ-Al_2O_3 catalyst, Appl. Catal. B: Environ. 147 (2014) 464–480.
[31] P. Hirunsit, C. Luadthong, K. Faungnawakij, Effect of alumina hydroxylation on glycerol hydrogenolysis to 1,2-propanediol over Cu/Al_2O_3: combined experiment and DFT investigation, RSC Adv. 5 (2015) 11188–11197.
[32] C. He, J. Zheng, K. Wang, H. Lin, J.-Y. Wang, Y. Yang, Sorption enhanced aqueous phase reforming of glycerol for hydrogen production over Pt-Ni supported on multi-walled carbon nanotubes, Appl. Catal. B: Environ. 162 (2015) 401–411.